

Acoustic emission and fatigue crack growth in rigid polyurethane foam

F. W. NOBLE

*Department of Metallurgy and Materials Science, University of Liverpool,
PO Box 147, Liverpool, UK*

Compact tension specimens of a rigid polyurethane foam have been tested in fatigue and crack growth has been monitored visually and by means of acoustic emission (AE). During the load cycle it has been found possible to resolve the AE activity into four regions: the crack faces "un-sticking", fracture events at or close to peak load, a period of zero AE just after peak load, and AE associated with crack closure lower down the unloading part of the cycle. The fracture AE has been found to increase rapidly with crack length – consistent with a seventh power dependence on ΔK – and to occur during every cycle at high ΔK values, but to be absent in an increasingly greater proportion of cycles as ΔK is decreased below about $40 \text{ kPa m}^{1/2}$. AE data obtained on samples in which crack growth occurred across the layers of foam, through the high density inter-layer skins, show that the technique is very sensitive to the crack retardation effect associated with these skins well before this retardation is detectable visually.

1. Introduction

It has been shown [1, 2] that fatigue crack growth in the rigid polyurethane foam with which this work is concerned can be analysed according to linear elastic fracture mechanics. In particular, at ambient temperatures, the rate of crack advance per cycle can be described by a modified version of the Paris Law [3, 4] incorporating both the stress intensity range in the fatigue cycle, ΔK , and the maximum stress intensity of the cycle, K_{\max} . The crack growth data to which this law was found to be applicable was obtained roughly in the range $40 \text{ kPa m}^{1/2} < \Delta K < 120 \text{ kPa m}^{1/2}$ and there was evidence from acoustic emission studies [5], as well as from the observed growth rates, that below $\Delta K = 40 \text{ kPa m}^{1/2}$, the rate of crack advance was lower than the Paris Law would predict. This behaviour was interpreted in terms of an approach to a threshold ΔK (at about $20 \text{ kPa m}^{1/2}$) below which fatigue crack growth ceased to occur.

The material in question has been developed by Shell Research Ltd., and is a closed cell foam with a density of 85 kg m^{-3} and an elastic modulus of 25 MN m^{-2} . The mean cell diameter is about $180 \mu\text{m}$. Because of the intended use of the

material as a load bearing insulant subjected to fluctuating loads, the observation that fatigue crack growth is amenable to treatment by fracture mechanics is significant but the detection of such cracks in this type of material poses problems. It is in this area that acoustic emission (AE) techniques appear to be applicable and it is with the use of this technique to monitor crack growth in this material that the present work is concerned.

2. Experimental method

The experimental method involved in testing the material and recording the AE activity during fatigue crack growth has been described in detail elsewhere [1, 2, 5] and may be summarized as follows. The material was cut into the form of compact tension (CT) specimens containing a cut 20 mm long starter crack and with $W = 60 \text{ mm}$ and $B = 30 \text{ mm}$, in the usual notation. The AE transducer was fixed to the top face of the CT specimen and its amplified output was recorded continuously during each cycle in terms of the total number of "ring-down" pulses emitted by the growing crack. Numerous tests showed that all the AE activity recorded could be associated

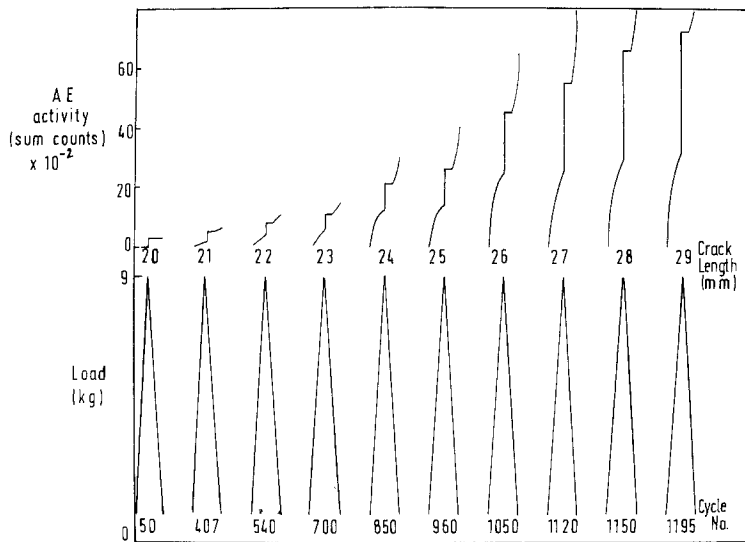


Figure 1 The development of the AE pattern with increase in crack length during cyclic loading for a sample loaded between 1 and 9 kg.

with the crack and no difficulty was experienced with spurious noise from the testing machine or gripping arrangement. Crack growth was monitored visually and ΔK was calculated as a function of crack length using an appropriate polynomial equation [6]. The rate of cycling during the fatigue tests was in the range 0.15 to 0.25 Hz, the applied load being positive at all times.

The foam was initially manufactured in the form of sprayed panels, the thickness of the panel being built up by a number of passes. Each pass produced a layer of foam about 10 mm thick and each layer was separated from its neighbour by a skin, about 0.15 mm thick, of high density material. In the previous studies on this material the CT specimens were cut such that the fatigue crack propagated between and parallel to the skins, in low density material. In the present work tests have also been performed on samples cut such that the fatigue crack propagated at right angles to the skins, i.e. across successive layers. In these specimens the starter crack was cut such that it just penetrated beyond one of the skins (by about 2 mm), the fatigue crack growth being monitored over the remaining 8 mm before the next skin was encountered.

3. Results

3.1. Crack growth parallel to the skins

The AE pattern associated with each cycle during fatigue crack growth was found to change as the fatigue crack developed from the starter crack and increased in length. This development of the AE pattern is illustrated in Fig. 1 which summarizes

the results obtained from a sampled cycled between 1 and 9 kg (an initial ΔK of $65 \text{ kPa m}^{1/2}$) as the crack increased in length from 20 to 29 mm. The crack length at which each AE pattern was observed is indicated beneath it and the relationship between each pattern and the cycle to which it relates is provided by the appropriate triangular waveform of that cycle, positioned beneath the AE figures.

In each cycle (including the first) a burst of AE activity was observed at, or close to, the peak load in the cycle. Before the fatigue crack has fully developed from the starter crack (within the first millimetre of growth) this is the only AE activity in the cycle, but after the crack has developed beyond this, additional AE occurs in both the unloading and loading parts of the cycle. Eventually the AE pattern stabilizes, and from $a = 23 \text{ mm}$ to $a = 29 \text{ mm}$ the form of the pattern is unchanged, though the magnitude of the emissions increases progressively with increase in crack length. The AE pattern associated with growth in this region is shown schematically in Fig. 2 and each identifiable part of the AE characteristic is labelled with the same letter as the part of the adjacent load cycle to which it relates. Region B, which corresponds to the region of the load cycle at and just before peak load, is identified as the AE arising from the fracture events associated with the fatigue crack advance at peak load, while regions A and D, following the interpretation of similar effects in metals [7, 8], are identified with the faces of the fatigue crack being either pressed together on unloading (region D) or being pulled

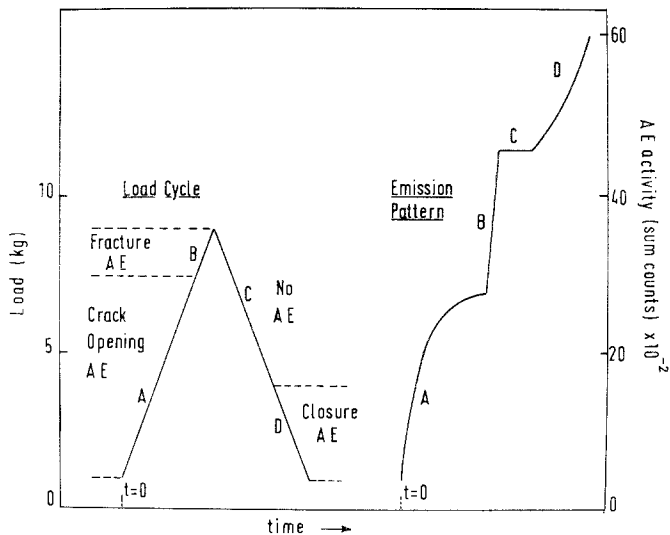


Figure 2 The relationship between the AE pattern and the various stages of the load cycle.

apart on loading (region A). The region of complete silence after peak load (region C) presumably results from the faces of the crack having been discontinuously displaced away from each other as a result of the peak load fracture and remaining apart (and hence silent) until well down the unloading part of the cycle when crack closure occurs (region D).

The variation of the magnitude of the AE activity with crack length is shown in Fig. 3 for two samples tested over the same load range, 6 kg, one between 4 and 10 kg the other between 1 and 7 kg. In this figure the term "fracture AE" refers to the magnitude of region B and the term "closure AE" to region D. The results indicate a similar monotonic dependence of fracture AE on

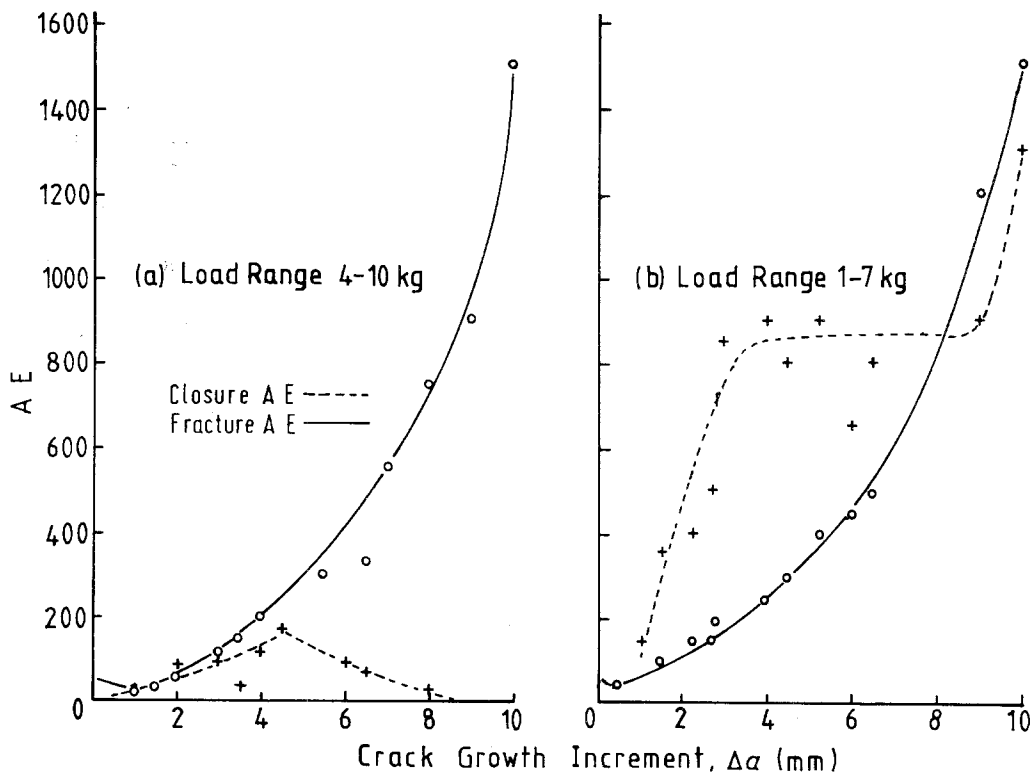


Figure 3 The variation of fracture AE and closure AE with crack length for specimens cycled from 4–10 kg and 1–7 kg, respectively.

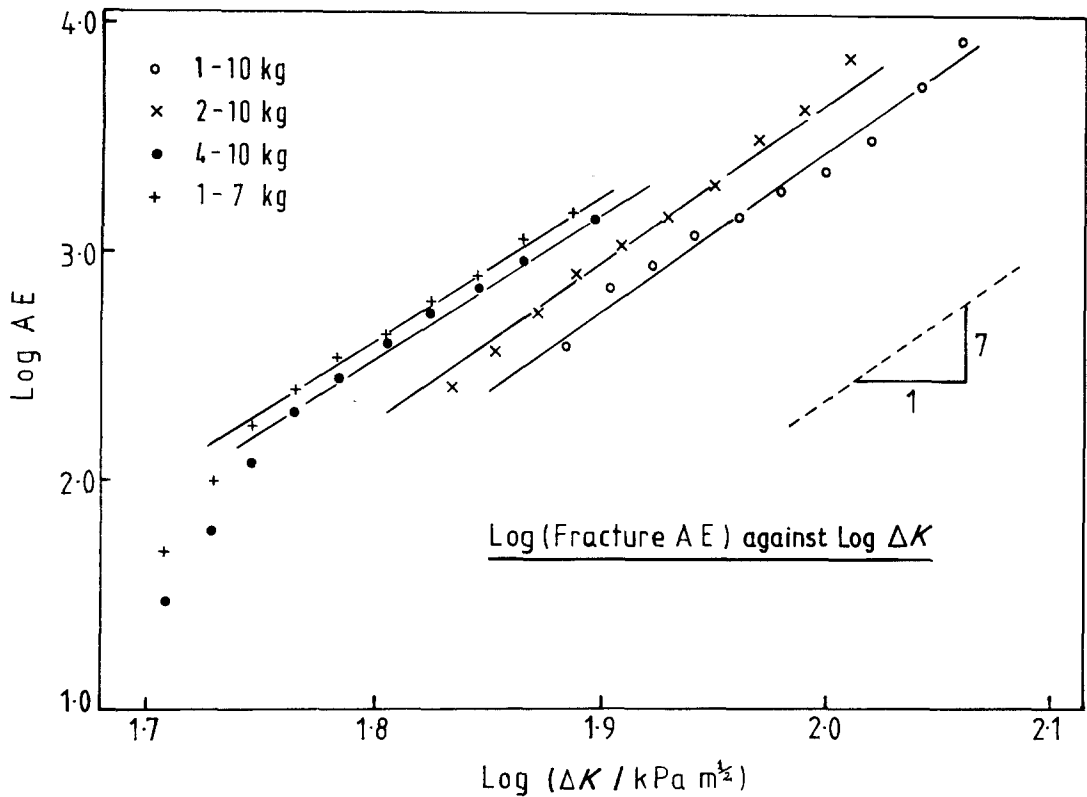


Figure 4 The variation of fracture AE with ΔK for four separate specimens.

crack length (at least after the first millimetre of growth) for both samples, though the crack closure AE behaves differently in each case. This presumably reflects the different R -ratios associated with the tests (0.4 compared with 0.14), the closure effect all but vanishing towards the end of the 4 to 10 kg test. However, in general it was found that the closure AE was not reproducible nor did it show any systematic variation from test to test.

The variation of fracture AE with crack length can more meaningfully be represented in terms of the ΔK increase associated with the change in length and this is illustrated by Fig. 4, in which the log of the fracture AE is plotted as a function of $\log \Delta K$ for the loading conditions indicated. For reasons to be considered later a linear relation was sought between \log (fracture AE) and $\log \Delta K$ and a line of slope equal to seven has been included in the figure for comparative purposes.

Provided the load range was sufficiently great, as in all the tests so far considered, fracture AE was observed in every cycle including the first but if the test was started at a sufficiently low load range, say 1 to 2 kg, then no fracture AE (or any

other AE) was detected. By retaining the lower load at 1 kg and progressively increasing the maximum load it was possible to assess the fracture AE activity by observing an appreciable number of cycles at each load range. This revealed that as the maximum load was increased the number of cycles which showed fracture AE progressively increased from zero until every cycle showed evidence of fracture. This effect is shown in Fig. 5, in which the fraction of cycles exhibiting fracture AE is plotted as a function of the ΔK value corresponding to each value of maximum load. The results indicate that below $201 \text{ kPa m}^{1/2}$ fracture activity is negligible while above $40 \text{ kPa m}^{1/2}$ it occurs in every cycle.

3.2. Crack growth perpendicular to the skins

The retarding effect of the interlayer skins on crack growth normal to them is illustrated in Fig. 6 for two samples tested between 1 and 10 kg. Although the growth rate in the sample showing crack growth perpendicular to the skins is initially larger than the sample with crack growth parallel to the skins (within the normal

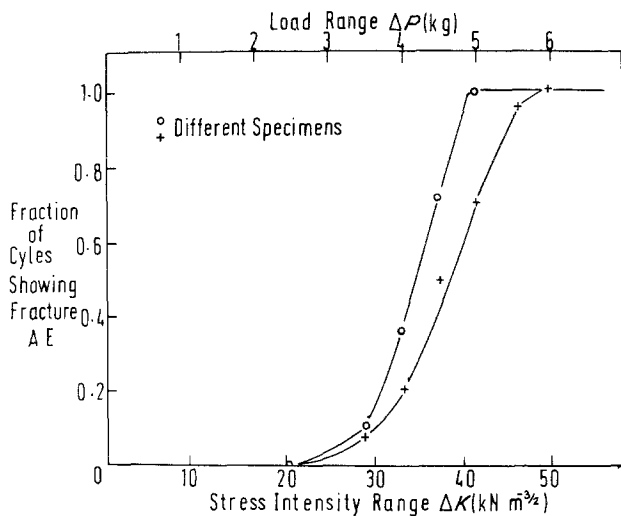


Figure 5 The fraction of cycles exhibiting fracture AE as a function of ΔK ($K_{min} = \text{constant}$).

scatter) the rate of growth in the former sample decreases markedly as the crack comes within about 2.5 mm of the skin and almost stops, the retardation effect being such as to eventually give both specimens similar lives in spite of the initial difference in growth rates. The position of the skin has been represented by a band in Fig. 6 (and Fig. 7) because of the uncertainty of fixing its position exactly by macroscopic surface measurement, and because, in general the skins were not completely planar and intersected the surfaces of the sample at slightly different positions on either side.

The retardation phenomenon is shown to greater effect by the AE data presented in Fig. 7 for the two samples to which Fig. 6 refers. Surprisingly the effect of the skin appears to extend well beyond the visually determined crack retardation in that the fracture AE hardly changes in the first 5 mm of growth perpendicular to the skin, in contrast to the three-fold increase recorded for the same change in crack length for growth parallel to the skins. This effect was also found in samples tested between 2 and 10 kg and 1 and 7 kg, respectively. The visually observed retardation appears, in fact,

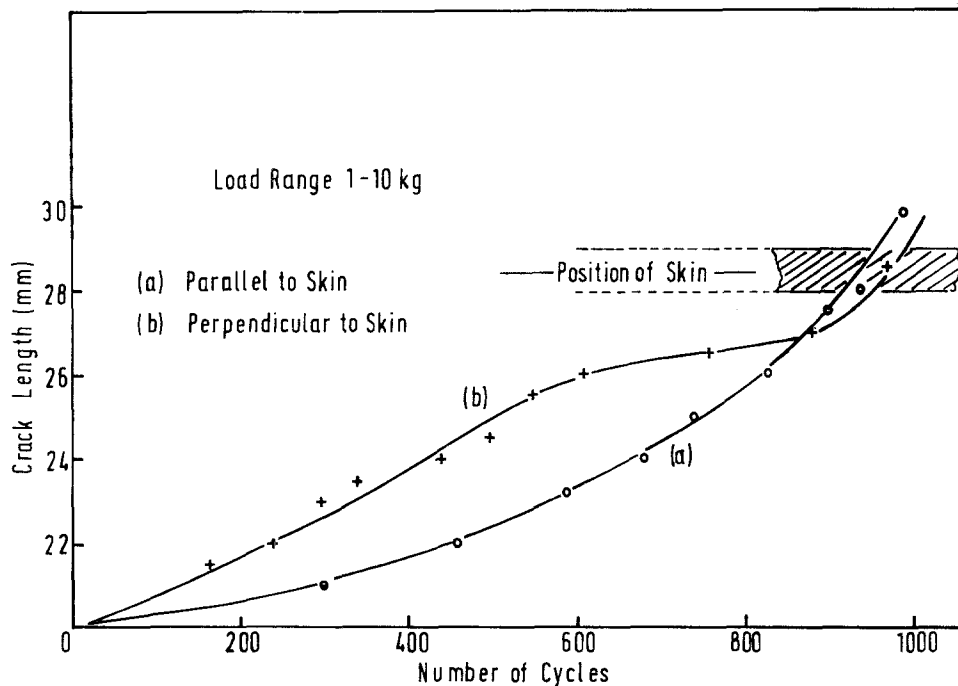


Figure 6 Crack growth behaviour: (a) for growth parallel to the skins; (b) for growth perpendicular to the skins.

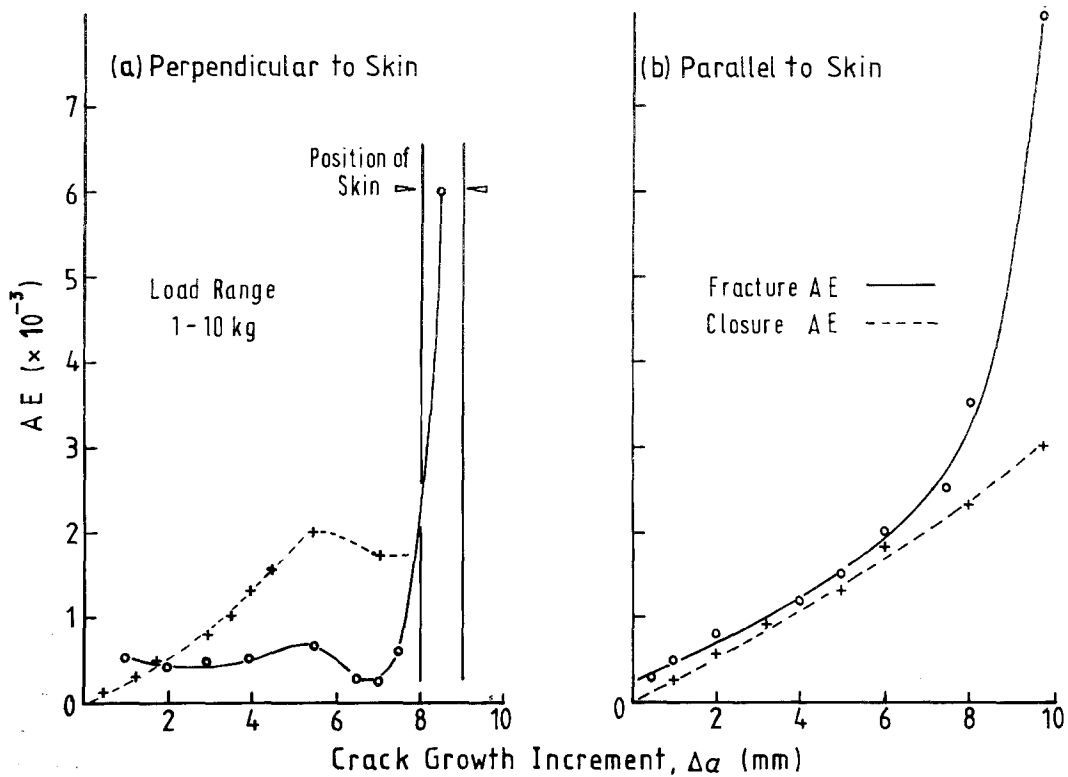


Figure 7 Comparison of fracture AE and closure AE as a function of crack growth increment: (a) for growth perpendicular to the skins (b) for growth parallel to the skins. (Same samples as in Fig. 6.)

to be accompanied by a decrease in fracture AE and final penetration of the skin was accompanied by a rapid increase in fracture AE which was detected well before surface observations of the crack's position indicated this event had occurred.

4. Discussion

4.1. Crack growth parallel to the skin

4.1.1. The variation of fracture AE with ΔK

The fracture AE may be assumed to be proportional to the crack advance per cycle, da/dN , in which case it should exhibit the same ΔK dependence as does the growth rate. In addition, however, the magnitude of the elastic energy released as AE as a consequence of the advance of the crack should also depend on the square of the stress intensity at which the release occurs, i.e. the square of the maximum stress intensity in the cycle, K_{\max}^2 . Since the crack growth rate in this material has been found to be given by [1]

$$\frac{da}{dN} = 2.85 \times 10^{-9} \frac{\Delta K^5}{(1-R)} \quad (1)$$

(ΔK in $\text{kPa m}^{1/2}$ and da/dN in $\mu\text{m cycle}^{-1/2}$) then

the fracture AE should be proportional to $[\Delta K^5 / (1-R)] K_{\max}^2$, i.e. to $[\Delta K^7 / (1-R)^3]$ since $K_{\max} = [\Delta K / (1-R)]$, where R is the load ratio of the fatigue cycle. This explanation of the ΔK dependence of the fracture AE has been advanced previously to account for the AE associated with fatigue crack growth in metals [8] and the linearity of the plots presented in Fig. 4 (at least at the higher ΔK values) and the closeness of their slopes to 7 indicate the extent of its applicability to the present material. In these plots no account has been taken of the $(1-R)$ dependence but if this is allowed for, as in Fig. 8, by replotting the lines drawn in Fig. 4 in terms of $\log [AE \times (1-R)^3]$ against $\log \Delta K$, the results of these tests at different R ratios are brought into closer coincidence. The data for the 1 to 7 kg test, however, remain displaced from the other data and indeed these data do appear anomalous in that the magnitude of the AE in the 1 to 7 kg test should be appreciably less than that recorded for the same crack growth rate in the test performed between 4 and 10 kg, because of the difference in peak load at which the fracture AE is generated. Since the visually observed crack growth rates were anomalously

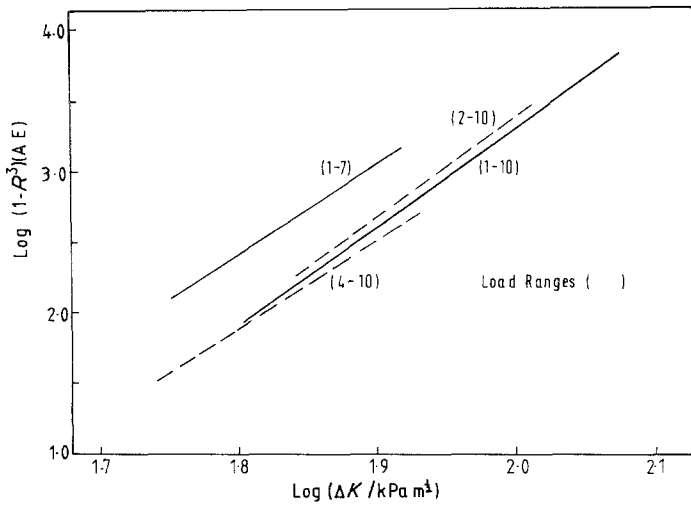


Figure 8 Log (fracture AE $\times (1 - R)^3$) against log ΔK . Data taken from the lines drawn through the points in Fig. 4.

high in the 1 to 7 kg test it would appear that the results from this specimen do not provide a fair test for evaluating the consistency of the AE behaviour from sample to sample.

4.1.2. The fracture process

The structure of the foam can be envisaged as a network of struts within which the roughly dodecahedral closed cells are formed by thin membranes of material stretched, between the appropriate struts to form the cell walls, each wall being roughly pentagonal [9]. Crack propagation in such a structure can be envisaged in terms of the failure of the struts at the tip of the crack, the membranes attached to the struts offering little resistance to crack growth but simply tearing, and "notching" the next strut to which they are attached at the end of the tear [10]. On this basis the AE at peak load can be associated with strut failure and the rate of crack advance will depend on the number of strut failures in each cycle.

In the range in which fracture AE is generated in each cycle, therefore, at least one strut is failing in each cycle and the region of the crack front at which a strut failure occurs will advance, roughly, by the inter-strut spacing. In subsequent cycles localized crack advance will occur at different positions along the crack front until after a sufficient number of cycles have elapsed the entire crack front will have advanced into the material. Examination of the fracture surface of the foam shows that the cross-section of the cells so revealed is roughly hexagonal with a failed strut at each corner of the hexagon, shared by the three

adjacent cells. Thus each failed cell is associated with two failed struts and for the entire crack front (30 mm wide) to advance by 1 cell diameter (about 180 μm) will require the failure of about 400 struts. If each cycle exhibiting fracture AE were assumed to involve just one strut failure the advance of the crack by one cell diameter would require 400 cycles and the observed (average) growth rate of the crack would be about 0.5 $\mu\text{m cycle}^{-1}$. Since, in general, more than one strut failure will occur in each cycle this figure represents the minimum growth rate consistent with the generation of fracture AE in each cycle. This figure is consistent with the growth rate predicted by Equation 1 for $\Delta K = 40 \text{ kPa m}^{1/2}$, the ΔK value below which the first non-emitting cycles occur and the deviations from the modified Paris Law become appreciable [1]. Obviously a larger number of strut failures per cycle, at larger ΔK values, will give higher growth rates but all the observed growth rates (before the onset of unstable growth) were less than 180 $\mu\text{m cycle}^{-1}$ implying that within the stress intensity ranges studied crack growth was always by non-uniform advance of the crack front.

The identification of fracture AE with the failure of individual struts or groups of struts implies that in the tests in which fracture AE is observed from the first cycle, "static" fracture must be occurring in that cycle — owing nothing to a fatigue process as such, though subsequent crack growth is fatigue controlled, as evidenced by its ΔK dependence [2]. The behaviour of the fracture AE associated with the development of the fatigue process is shown in Fig. 9, the fracture AE

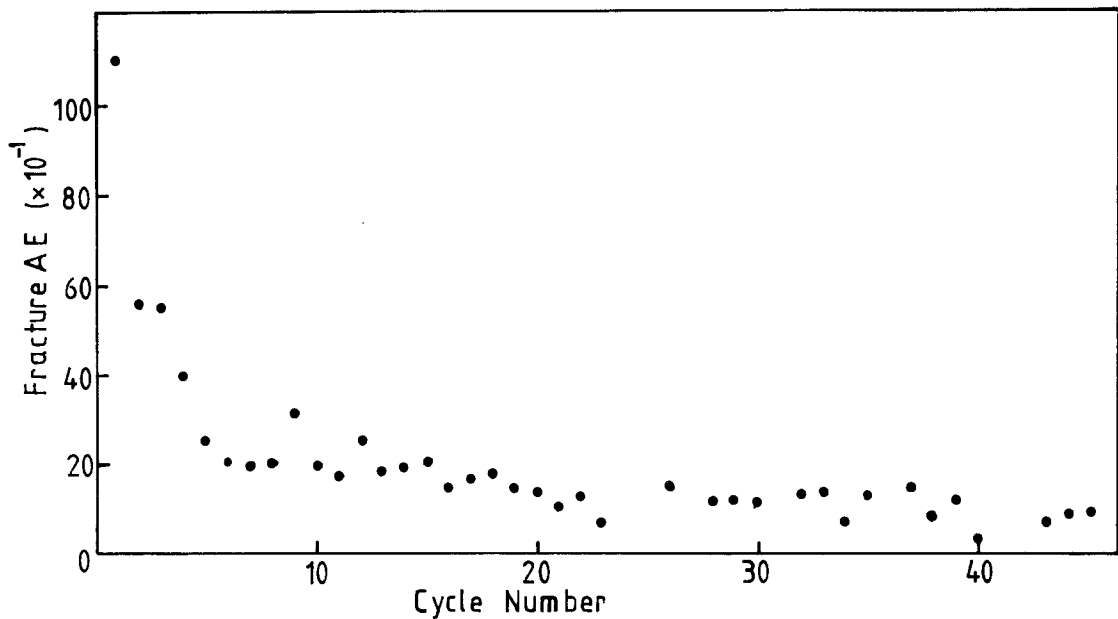


Figure 9 The fracture AE recorded in the first 45 cycles of the specimen cycled between 4 and 10 kg.

decreasing during the first 50 cycles (of the 4 to 10 kg test) before the monotonic increase shown in Fig. 3 takes effect, when the fatigue crack is fully established. The continued growth of the crack by a fatigue process must involve the production of irreversible damage at the crack tip which enables fresh fracture to occur during the subsequent cycle and this must happen both in the AE generating cycles (at the higher ΔK 's) and in the quiescent cycles between AE generating cycles (at the lower ΔK 's). A possible mechanism for the production of such damage is the buckling of unbroken struts at the crack tip under the compressive stresses generated there during the unloading part of the cycle. These buckled struts will either fracture at the peak load in the next cycle (being unable to accommodate the imposed opening displacement at the crack tip) or will modify the deformation pattern at the crack tip during the next cycle. On the other hand there may well be an element of continuous, non-AE generating crack growth associated with the deepening of the notches in the struts associated with membrane tearing which may progress cyclically until the strut is so deeply notched as to fracture on the next load application.

4.2. Growth perpendicular to the skin

The AE results for crack growth perpendicular to the skins probably reflect two different effects. In the early stages of growth the material at the

crack tip and in the "damage" zone ahead of the tip is the low density cellular material and the only effect the skin will be expected to have will be through the stiffening effect it exerts on the neighbouring foam. This will result in a reduction in the stress intensity at the crack tip relative to the same crack in unstiffened material. The AE results appear to show that the increase in the stiffening effect as the skin is approached balances out the increase in ΔK associated with increase in crack length to result in a nearly constant AE and hence growth rate in this region. Eventually the damage zone, which can be estimated as about 2 mm in extent [2], will encompass the high density material of the skin, at which point the decrease in crack growth rate will reflect the changing material properties, and the decrease in AE in this region cannot simply be regarded as a decrease in ΔK due to stiffening. Eventual penetration of the skin results in a virtual removal of both the retardation effects, the crack now propagating through low density cellular material sufficiently distant from the next skin as to minimize stiffening effects, and there is a rapid increase in crack growth rate and fracture AE emissions, leading to fast, unstable fracture. Indeed, it was noticeable that whereas final fracture produced by cracks parallel to the skins occurred by tearing and required a continuous movement of the crosshead on the tensile machine, final fracture in the specimens with cracks running

across the skins was unstable and far more brittle in character. So although the initial crack in fatigue is retarded in the latter specimens by the skin, final fracture, once the crack is large enough, appears more catastrophic.

Acknowledgements

The authors would like to thank Professor Schaarwächter and Herr H. Ebener of Dortmund University for the provision of the testing equipment and Shell Research Ltd., for their assistance in carrying out the work.

References

1. F. W. NOBLE and J. LILLEY, *J. Mater. Sci.* **16** (1981) 1801.
2. J. LILLEY, MSc thesis, University of Liverpool (1980).

3. A. C. PARIS and F. ERDOGAN, *J. Bas. Eng.* **85** (1963) 528.
4. R. ROBERTS and F. ERDOGAN, *ibid.* **89** (1967) 885.
5. F. W. NOBLE, Conference Proceedings on Fatigue Thresholds, Stockholm, 1981, Vol. 2 (Engineering Materials Advisory Services, Warley, 1982).
6. J. E. STRAWLEY, *Int. J. Fract.* **12** (1976) 475.
7. T. M. MORTON, R. M. HARRINGTON and J. G. BJELETICH, *Eng. Fract. Mech.* **5** (1973) 691.
8. T. C. LINDLEY, I. G. PALMER and C. E. RICHARDS, *Mater. Sci. Eng.* **32** (1978) 1.
9. J. R. DAWSON and J. B. SHORTALL, *J. Mater. Sci.* **17** (1982) 220.
10. T. COTGREAVE and J. B. SHORTALL, *J. Cell. Plastics* **13** (1977) 240.

*Received 6 October
and accepted 23 November 1982*